

The Li isotopic composition of Oldoinyo Lengai: Nature of the mantle sources and lack of isotopic fractionation during carbonatite petrogenesis

Ralf Halama^{a,*}, William F. McDonough^a, Roberta L. Rudnick^a,
Jörg Keller^b, Jurgis Klaudius^b

^a *Geochemistry Laboratory, Department of Geology, University of Maryland, College Park, MD 20742, U.S.A.*

^b *Mineralogisch-Geochemisches Institut, Albert-Ludwigs-Universität Freiburg, Albertstr. 23b, 79104 Freiburg, Germany*

Received 19 May 2006; received in revised form 3 November 2006; accepted 13 November 2006

Available online 21 December 2006

Editor: Dr. R.W. Carlson

Abstract

Lithium concentrations and Li isotope compositions are reported for natrocarbonatites and silicate lavas from Oldoinyo Lengai, Tanzania. Natrocarbonatites are characterized by very high Li contents (211–294 ppm) and a narrow range of $\delta^7\text{Li}$ values between +3.3 and +5.1. These Li isotope compositions overlap with those reported for MORB and OIB and suggest that the natrocarbonatites reflect the Li isotopic composition of their mantle source. Co-genetic silicate lavas, covering a wide compositional spectrum, show no obvious isotopic fractionation as a function of igneous differentiation or liquid immiscibility. Primitive olivine melilitites ($\text{Mg}\# = 58\text{--}70$), considered to be parental magmas, contain 14–23 ppm Li and have $\delta^7\text{Li}$ values of +2.4 to +4.4. A highly differentiated, peralkaline nephelinite ($\text{Mg}\# = 12$), likely to be related to the natrocarbonatites by liquid immiscibility, has about twice as much Li as the melilitite (57 ppm), but a similar isotopic composition ($\delta^7\text{Li} = +3$). In contrast, a phonolite with 15 ppm Li has a lighter Li isotope composition ($\delta^7\text{Li} = -0.4$), which may reflect assimilation of isotopically light lower crustal mafic granulites, a conclusion supported by radiogenic isotope data. Clinopyroxene and olivine separates from the silicate lavas have uniformly lower Li concentrations (3–15 ppm) and lower $\delta^7\text{Li}$ values ($\delta^7\text{Li} = -2.9$ to -0.5) than the respective whole-rocks, with $\Delta^7\text{Li}_{\text{whole-rock-mineral}}$ between 1.4 and 6.3. This difference between whole-rock and mineral data is interpreted to reflect diffusion-driven isotopic fractionation.

© 2006 Elsevier B.V. All rights reserved.

Keywords: Lithium isotopes; Carbonatites; Oldoinyo Lengai; Mantle geochemistry

1. Introduction

Lithium is a fluid-mobile alkali metal that is incompatible during mantle partial melting [1]. The significant

mass difference ($\sim 16\%$) between its two stable isotopes, ^6Li and ^7Li , produces a large isotopic fractionation in low temperature terrestrial systems [2]. Therefore, Li isotopes have the potential to be effective tracers of surface material recycled into the mantle [3] and Li isotope studies of mantle-derived igneous rocks have predominantly focused on oceanic and subduction zone settings to detect a geochemical signature thereof.

* Corresponding author. Tel.: +1 301 405 2707; fax: +1 301 405 3597.

E-mail address: rhalama@geol.umd.edu (R. Halama).

Fresh mid-ocean ridge basalts (MORBs) have $\delta^7\text{Li}$ values from 1.6 to 5.6 [4–7] ($\delta^7\text{Li} = 1000 \times [{}^7\text{Li}/{}^6\text{Li}_{\text{sample}}/{}^7\text{Li}/{}^6\text{Li}_{\text{standard}} - 1]$, using the standard L-SVEC [8]). The $\delta^7\text{Li}$ values of ocean-island basalts (OIBs) ($\delta^7\text{Li} = +3$ to $+7$ [9–12]) generally overlap with the range determined for MORB. OIB associated with the HIMU (high μ , $\mu = {}^{238}\text{U}/{}^{204}\text{Pb}$) mantle isotopic signature may show relatively heavy values ($\delta^7\text{Li} = +5.0$ to $+7.4$) [11,12]. The elevated $\delta^7\text{Li}$ values in both HIMU and some arc lavas were interpreted to reflect the incorporation of Li from altered oceanic crust [6,12], but the generally poor correlations with other fluid-mobile elements in arc lavas suggest that Li from the subducting slab may be removed from fluids and melts during mineral/fluid equilibration in the subarc mantle [13,14]. For intraplate igneous rocks from continental settings, Li isotope data are still scarce. Basaltic rocks from Antarctica show Li isotopic signatures very similar to the oceanic rocks ($\delta^7\text{Li} = +3$ to $+5$), with both higher and lower values for more evolved samples [11], and a single alkali-syenite from NE Mexico has $\delta^7\text{Li} = +2.1$ [15]. The relatively small range in $\delta^7\text{Li}$ of mantle-derived magmas contrasts with data from mantle xenoliths, where the range of $\delta^7\text{Li}$ is considerable (-17 to $+12$) [16–18].

Li isotopes do not show mass fractionation at a per-mil level during differentiation at high temperatures (>1050 °C) in basaltic magmas [10] and during crustal anatexis [19,20]. However, significant fractionation of Li isotopes occurs during extreme granite differentiation and pegmatite formation at temperatures of 340–600 °C [21], during seafloor alteration at temperatures ≤ 350 °C [22,23], weathering [24,25] and metamorphic dehydration [14,26]. Additionally, high temperature diffusion during magma wall-rock interaction [27,28] and degassing [29] can also produce significant Li isotope fractionation. At present, it is not established whether igneous differentiation of alkaline magmas can produce Li isotopic fractionation.

Here we report Li concentrations and Li isotopic signatures of carbonatitic and silicate lavas from Oldoinyo Lengai, Tanzania. Based on Sr–Nd–Pb isotopes, Bell and Tilton [30] proposed that the Lengai rocks represent a mixture of the EM1 and HIMU mantle components and should therefore provide clues to the Li isotopic composition of these components. The range of eruption temperatures, from >1100 °C (olivine melilitites [31]) to 490 °C (natrocarbonatites [32,33]), provide a critical test case for Li isotope fractionation during magmatic differentiation in these systems. Additionally, a comparison of whole-rocks to clinopyroxene separates from the silicate lavas provides information on Li isotope fractionation in mineral-melt systems.

2. Analytical procedures

Whole-rock powders are the same as those investigated in previous studies [34–36] and all analyses reported here were carried out at the University of Maryland. Clinopyroxene mineral separates were obtained by using a magnetic separator, followed by hand-picking from fractions in the 180–315 μm mesh size. Before dissolution, mineral separates were cleaned by ultrasonic bathing (15 min) in Milli-Q water (18.2 M Ω cm). Separates are estimated to be $>98\%$ pure. Acid digestion of rock powders (5–20 mg) and mineral separates as well as column chemistry methods employed in this study follow the procedures described in [24]. A minor modification was the introduction of an additional refluxing step with aqua regia during sample digestion. This step was found useful for obtaining clear solutions before the final digestion in concentrated HCl. Details of the instrumental analysis are given in [20]. Each sample analysis is bracketed before and after by measurement of the L-SVEC standard and the $\delta^7\text{Li}$ value of the sample is calculated relative to the average of these two bracketing L-SVEC runs. Two standard solutions, IRMM-016 [37] and the in-house UMD-1 standard (a purified Li solution from Alfa Aesar[®]) were routinely analyzed during the course of an analytical session. The results for both (IRMM-016: $+0.2 \pm 0.8\%$ (2σ), $n=18$; UMD-1: $54.7 \pm 1.0\%$ (2σ), $n=24$) agree well with published results (IRMM-016: -0.1% [37], $-0.1 \pm 0.2\%$ [24]; UMD-1: $+54.7 \pm 1\%$ [20,24]). Analyses of the international rock standard BHVO-1 gave $+4.4 \pm 0.7\%$ ($n=7$) compared to previously published values between $+4.3$ and $+5.8$ [9,24,38,39]. We typically measure a voltage of 2–3 V for ${}^7\text{Li}^+$ ions for a solution with 50 ppb Li and a 40 $\mu\text{l}/\text{min}$ solution uptake rate. For comparison, the total procedural blank yields 20–40 mV for mass 7, resulting in a sample/blank ratio of ~ 40 . With $\delta^7\text{Li} \sim -19$, the blank influence is negligible at the present level of precision ($\pm 1\%$, 2σ). Li concentrations were determined by comparing signal intensities of sample solutions with 50 ppb L-SVEC and then adjusting for sample weight. The accuracy of this method was established by Teng et al. [20], and the uncertainty is $< \pm 10\%$ [28].

For C and O isotopic analyses, 0.1–0.2 mg sample powder was placed in a vial in a heated sample tray attached to a Gilson autosampler. A double hole needle design allows initial pumpout of the samples, introduction of phosphoric acid, and transfer of the resulting CO_2 into the dual inlet system. Water is removed using a cryogenic probe operating at -70 °C, and the CO_2 sample is collected using an external liquid nitrogen cold-finger.

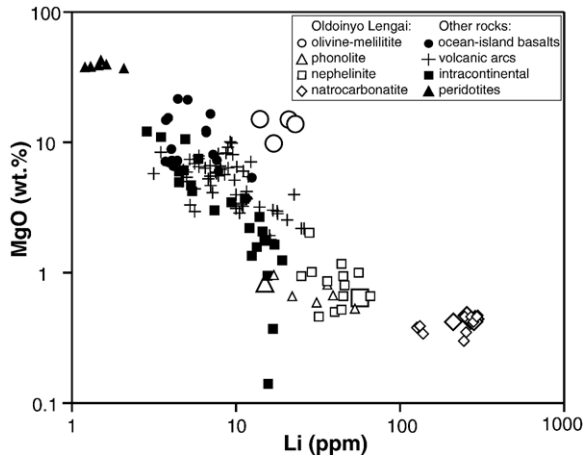


Fig. 1. Li vs. MgO abundances of Oldoinyo Lengai rocks compared to rocks from various tectonic settings. Large symbols are samples analyzed in this study, additional data for Oldoinyo Lengai are from [36,59]. Other data sources: [5,6,10–13,73–77].

Measurements were performed on a Micromass Multi-Prep mass spectrometer. C and O isotope compositions are reported in the standard δ -notation relative to PDB and V-SMOW, respectively. Sample analyses are bracketed by repeat analyses of the NBS-19 carbonate standard, which gave $\delta^{13}\text{C}_{\text{PDB}}=2.73\pm 0.14$ (2σ , $n=7$)

and $\delta^{18}\text{O}_{\text{V-SMOW}}=28.50\pm 0.16$ (2σ , $n=7$). Sample values were corrected for the offset from the accepted values ($\delta^{13}\text{C}_{\text{PDB}}=1.95$ and $\delta^{18}\text{O}_{\text{V-SMOW}}=28.6$).

In situ Li concentration analyses of pyroxenes and olivines on grain mounts were performed using a New Wave UP-213 laser coupled to a ThermoFinnigan Element2 ICP mass spectrometer. A 65 μm spot was used with a repetition rate of 12 Hz. Output power was 45%, corresponding to ca. 4 J cm^{-2} . NIST 610 glass [40] was used for instrument calibration. Total acquisition time was 80 s per analysis, allowing about 20 s for background followed by 60 s for laser ablation. Mn was used as an internal standard to correct the ablation yield differences between and during individual analyses on both standards and samples. Multiple analyses of the reference basaltic glass BCR-2 g gave 9.6 ± 1.0 ppm Li (2σ , $n=9$), corresponding to an internal precision of $\pm 10.8\%$. This value falls in between published analyses of BCR-2 g (7.5 to 9.98 ppm Li [41]).

Mineral chemical compositions were determined using a JEOL JXA-8900 electron microprobe, operated with an acceleration voltage of 15 kV, a 10 nA beam current and a 5 μm beam size. Various natural mineral standards were used for calibration, and a ZAF correction was applied. Measuring times on the peak

Table 1
Li concentrations, Li–C–O isotope data and selected geochemical parameters of Oldoinyo Lengai rocks

Sample	Rock type	Material	Li ppm	$\delta^7\text{Li}$ (‰)	2σ	n	$\Delta^7\text{Li}_{\text{WR-mineral}}$	$\delta^{13}\text{C}_{\text{PDB}}$ (‰)	$\delta^{18}\text{O}_{\text{V-SMOW}}$ (‰)	SiO_2 (wt.%)	MgO (wt.%)	Mg#	PI
OL 123	Natrocarbonatite	WR	211	+4.8				−7.0	8.6	0.44	0.42		
OL 148	Natrocarbonatite	WR	292	+4.4				−7.0	7.4	n.d.	0.44		
OL 148 _{Replicate}	Natrocarbonatite	WR	283	+4.8	1.6	3							
OL 259	Natrocarbonatite	WR	244	+4.9				−6.9	7.4	0.23	0.43		
OL 259 _{Replicate}	Natrocarbonatite	WR	294	+5.1									
OL-2	Natrocarbonatite	WR	282	+3.6				−6.9	9.2	0.21	0.42		
OL-7	Natrocarbonatite	WR	255	+3.3				−7.0	9.3	0.10	0.47		
OL 352	Olivine melilitite	WR	21	+3.5						36.38	14.92	70.3	1.10
OL 352 _{Replicate}	Olivine melilitite	WR	21	+3.3	0.9	2							
OL 352 px	Olivine melilitite	Cpx	5.0	−2.9	0.7	2	6.3						
OL 352 ol	Olivine melilitite	OI	2.9	0.0			3.4						
OL 198	Olivine melilitite	WR	23	+4.3						36.48	13.78	68.7	1.28
OL 343	Olivine melilitite	WR	14	+2.4						36.35	15.04	69.8	1.20
OL 12/2K	Olivine melilitite	WR	17	+4.4						34.07	9.80	58.7	1.74
OL 804	Nephelinite	WR	47	+3.1	0.8	2				45.51	0.64	12.1	2.33
OL 804 _{Replicate}	Nephelinite	WR	67	+2.8	2.1	2							
OL 804 px	Nephelinite	Cpx	8.6	−0.5	1.0	2	3.5						
OL 804 px _{Replicate}	Nephelinite	Cpx	8.4	−1.0	0.5	2	4.0						
OL 822	Phonolite	WR	16	−0.2						50.01	0.83	23.6	1.25
OL 822 _{Replicate}	Phonolite	WR	14	−0.6	0.9	2							
OL 822 px	Phonolite	Cpx	12	−1.8	0.9	2	1.4						

WR = whole-rock, Cpx = Clinopyroxene separate, OI = Olivine separate, n = Number of analyses of which average value is reported, PI = Peralkalinity index = $(\text{K} + \text{Na}) / \text{Al}$, Mg# = $\text{Mg} / (\text{Mg} + \text{Fe}^{2+})$ with $(\text{Fe}_2\text{O}_3 / \text{FeO} = 0.15)$. SiO_2 and MgO contents, PI and Mg# are from [34–36]; n.d. = not detected.

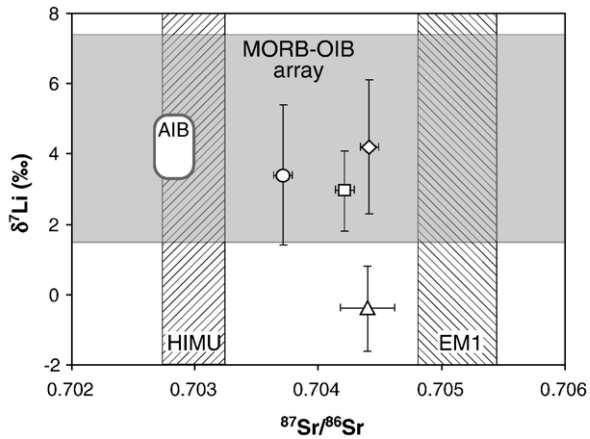


Fig. 2. Li–Sr isotope diagram showing Oldoinyo Lengai samples in comparison to mantle-derived lavas (MORB, OIB, intracratonic basalts). Symbols (as in Fig. 1) represent average values, error bars represent the range of measured values plus the external 2σ error ($\pm 1\%$). The field for AIB (= Antarctic Intraplate Basalt) is from [11]. Sr isotope data for OL rocks are from [34,51]. Hatched bars represent approximate Sr isotope ratios for HIMU and EM1 mantle components (after [78]).

positions varied between 10 and 60 s depending on the element analyzed.

3. Geological setting and sample description

Oldoinyo Lengai (OL), located in the East African Rift Valley in northern Tanzania, is the world's only

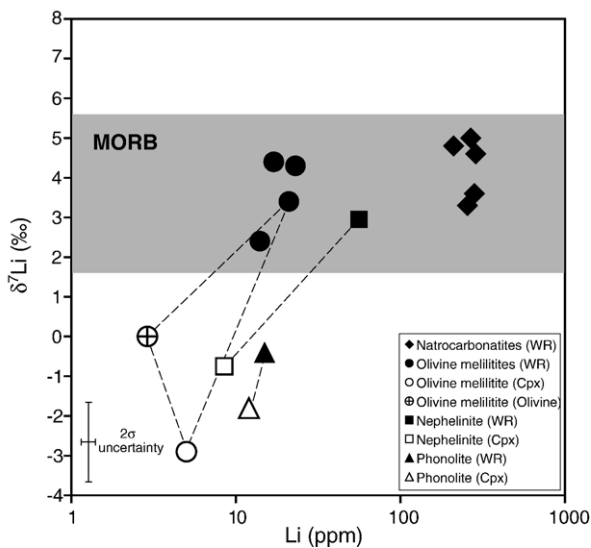


Fig. 3. Li isotopic compositions of Oldoinyo Lengai rocks and minerals plotted against Li concentrations. The dashed lines connect analyses of whole-rock and separated minerals from the same sample. For replicate analyses, the average value is plotted. The grey bar represents the composition of glassy MORB lavas [7].

active carbonatite volcano and represents the youngest manifestation of alkaline activity related to the East African rift system. Most of the volcano is composed of phonolitic and nephelinitic lavas, tuffs and agglomerates, but eruption of natrocarbonatites has been the dominant activity in this century [42]. Although olivine-bearing rocks, which might correspond to parental magmas, are rare or absent at Oldoinyo Lengai, unusually peralkaline olivine melilitites have erupted at several nearby, young volcanic centers [34,42]. The parental olivine melilitite magmas are thought to have evolved via crystal fractionation of olivine and melilitite to nephelinitic compositions [43]. Many workers think that the natrocarbonatites formed by liquid immiscibility from a carbonated nephelinitic magma [43–46]. On the basis of chemical data and field relationships, Keller and Spettel [45] favored an immiscible liquid separation of natrocarbonatites from a hyperalkaline combeite ($\text{Na}_2\text{Ca}_2\text{Si}_3\text{O}_9$) nephelinite. On the other hand, low-temperature (0.5–3.75 kbar, 700–850 °C) experiments

Table 2

Mineral chemical and *in situ* Li concentration data of Oldoinyo Lengai rocks

Grain #	Analysis area	Mg#	Na p.f.u.	Li (ppm) laser analyses*	Li (ppm) solution analyses*
Olivine grains from olivine melilitite (OL 352)					
1	Rim	0.87	–	3.1	
1	Core	0.86	–	2.8	
1	Interior	0.86	–	3.2	2.9
1	Rim	0.87	–	3.7	
7	Rim	0.86	–	1.4	
7	Core	0.81	–	2.6	
Clinopyroxene grains from olivine melilitite (OL 352)					
1	Core	0.83	0.04	0.8	
3	Interior	0.84	0.05	0.4	
3	Interior	0.84	0.05	1.0	
5	Interior	0.85	0.09	4.1	
5	Interior	0.86	0.03	6.8	
5	Interior	0.77	0.11	14.2	5.0
5	Interior	0.87	0.09	4.0	
10	Rim	0.71	0.21	4.9	
10	Interior	0.74	0.22	2.6	
10	Core	0.75	0.23	2.7	
10	Interior	0.78	0.21	3.7	
10	Rim	0.73	0.22	1.6	
Clinopyroxene grains from nephelinite (OL 804)					
10	Rim	0.57	0.20	2.8	
10	Interior	0.57	0.20	3.1	8.6
10	Core	0.60	0.20	3.5	8.4
Clinopyroxene grains from phonolite (OL 822)					
10	Rim	0.50	0.30	10.3	
10	Interior	0.58	0.28	5.9	12
10	Core	0.55	0.26	10.4	

* 2σ uncertainties of laser and solution analyses are $\pm 11\%$ and $\pm 10\%$, respectively.

suggest that immiscible, alkali-rich carbonatitic liquids are generated from wollastonite nephelinites at high P_{CO_2} , whereas combeite-bearing nephelinite is produced as a residual melt by prolonged fractionation under low P_{CO_2} [46]. Other proposed origins for the natrocarbonatites include differentiation of an alkalic olivine sövite magma under low $f_{\text{H}_2\text{O}}$ [47] and partial melting of fenitised lower crust [48]. Nielsen and Veksler [49] suggested that the natrocarbonatites are a cognate, mobile, alkaline and CO_2 -rich fluid condensate. Whatever the ultimate origin of the natrocarbonatites, and despite their highly evolved character, mantle source characteristics appear to be reflected in their C- and O isotope ratios [50], radiogenic isotope ratios [51] and certain trace element ratios (e.g. Ce/Pb and Th/Nb) [36].

The samples analyzed here comprise five natrocarbonatites (two from the 1993 eruption, one from the 1995 eruption and two from the 2000 eruption), four olivine melilitites from nearby cones (Sinja Lalarasi, Dorobo and Armykon Hill), a highly evolved wollastonite-bearing combeite nephelinite and a phonolite

from the oldest unit of Oldoinyo Lengai [35,52]. Clinopyroxene is the only phenocryst phase common to all three silicate rocks. More detailed sample descriptions are given in the Appendix.

4. Results

There is a first order negative correlation between Li and MgO contents for igneous rocks worldwide (Fig. 1). The olivine melilitites are enriched in Li (14–23 ppm) compared to lavas with similarly high MgO contents (<10 ppm Li). The more evolved silicate lavas from Oldoinyo Lengai follow the general trend. However, there is a notable enrichment of Li in the natrocarbonatites (130–300 ppm Li) compared to silicate rocks at similarly low MgO contents.

The Li isotopic compositions of the natrocarbonatites ($\delta^7\text{Li} = +3.3$ to $+5.1$, Table 1) are indistinguishable from values determined for average mantle, MORB, OIB and intracontinental basalts (Fig. 2). Within uncertainties, the compositions of these lavas overlap with the co-

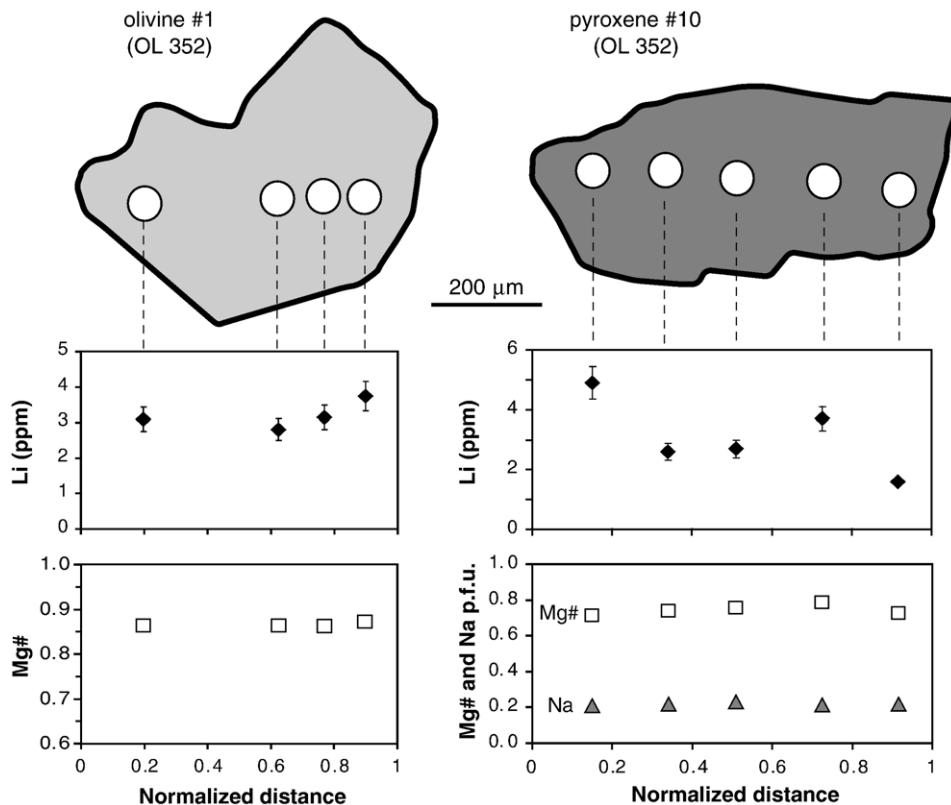


Fig. 4. *In situ* Li concentration analyses in olivine and pyroxene phenocrysts from an olivine melilitite. The sketch drawings of the minerals show the locations of the laser spots. Mg# and Na p.f.u. (per formula unit) were determined by electron microprobe. Error bars for Li represent the 2σ internal precision ($\pm 11\%$).

genetic olivine melilitites ($\delta^7\text{Li}=+2.4$ to $+4.4$) and the nephelinite ($\delta^7\text{Li}=+3$). The phonolite has a distinctly lighter Li isotopic signature ($\delta^7\text{Li}=-0.4$). Clinopyroxene separates from three silicate lavas have lower $\delta^7\text{Li}$ values than their respective whole-rocks (Fig. 3). The difference $\Delta^7\text{Li}_{\text{WR-cpx}}$ ($=\delta^7\text{Li}_{\text{whole-rock}}-\delta^7\text{Li}_{\text{cpx}}$) is small and within analytical uncertainties for the phonolite ($\Delta^7\text{Li}_{\text{WR-cpx}}=1.4\text{‰}$), but significant for both the nephelinite ($\Delta^7\text{Li}_{\text{WR-cpx}}=3.8\text{‰}$) and the olivine melilitite (sample OL 352; $\Delta^7\text{Li}_{\text{WR-cpx}}=6.3\text{‰}$). An olivine separate ($\Delta^7\text{Li}=0$) from sample OL 352 has also a lighter Li isotopic composition than the whole-rock.

Mineral chemical parameters and Li concentration data of pyroxene and olivine phenocrysts are presented in Table 2. Li concentrations measured by laser ICP-MS overlap with solution measurements for 3 of the 4 samples. The misfit in sample OL 804 may be explained by the limited amount of laser data that do not represent the range of Li concentrations occurring in the sample. Li concentrations appear to be uncorrelated to the mineral chemical parameters Mg# and Na p.f.u. (Fig. 4). Olivine #1 (sample OL 352), which is one of the largest crystals analyzed, shows a small decrease of Li from the rim to the core, although there is some overlap within uncertainty. A significantly higher Li concentration in one crystal rim compared to the core occurs in pyroxene #10 (sample OL 352). However, other crystals, mostly smaller than olivine #1 and pyroxene #10, show fairly constant Li distributions (e.g. pyroxene #10 in sample OL 804) or higher Li contents in the core than in the rim (e.g. olivine #7 in sample OL 352).

5. Discussion

5.1. Sample freshness

Since Li is fluid-mobile, it can be redistributed by metasomatic and weathering processes. The natrocarbonatites were sampled directly after eruption, so effects of weathering can be excluded. Additionally, C and O isotopic values ($\delta^{13}\text{C}=-6.9$ to -7.0 , $\delta^{18}\text{O}=+7.4$ to $+9.3$) fall into the field characterizing primary magmatic carbonatites (Fig. 5), confirming that they were not significantly affected by low-T alteration. Three samples have slightly elevated $\delta^{18}\text{O}$ values compared to the box defining primary values for Lengai carbonatites [53]. This may indicate incipient oxygen isotope exchange, which is most likely due to rapid isotopic alteration by equilibration with atmospheric humidity, a process that can even affect samples stored indoors [53]. However, it does not change Li isotopic compositions. Both Li and C isotopic compositions do not show a difference be-

tween these higher $\delta^{18}\text{O}$ samples and the “fresh” natrocarbonatites and are thus considered to be pristine.

For the silicate rocks, the freshest available materials (see [35] for details) were chosen for analyses. There is little petrographic evidence for weathering, except for a few altered combeite crystals in sample OL 804 [35], but mafic phenocrysts appear pristine.

5.2. Li enrichment

Li is usually incorporated into mantle minerals at the ppm level [54–56], and the bulk Li content of the MORB source and lithospheric mantle has been estimated to be between 1.0 and 1.8 ppm [1,55,57]. Mineral-melt partition coefficients for Li fall in the range 0.13–0.35 [1,58]. The relatively high Li contents of the olivine melilitite (>10 fold enrichment compared to average mantle) is consistent with this rock having formed via relatively small degrees of partial melting of the mantle [34]. Li enrichment in the natrocarbonatites (~ 150 fold enrichment compared to average mantle) may not only reflect the high degree of differentiation, but also a possible preference of Li for the carbonatitic melt during immiscible liquid separation. Assuming that the whole-rocks approximate the Li concentrations of the carbonate and silicate liquids, literature data [36,59], combined with our results indicate that the Li distribution coefficient of carbonatitic ($n=13$) versus nephelinitic ($n=14$) lava is, on average, ~ 5.5 .

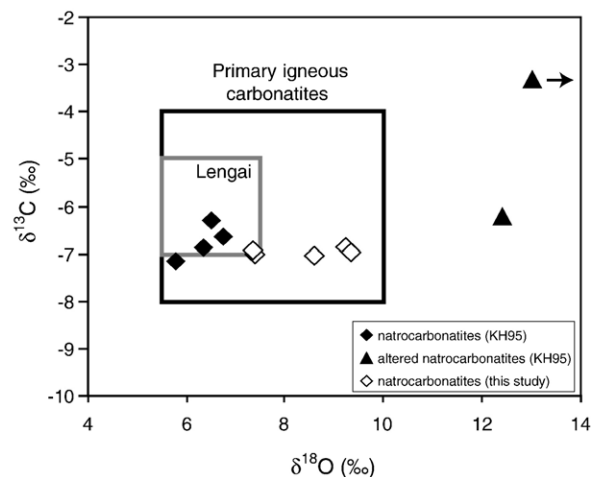


Fig. 5. C–O isotope plot for the natrocarbonatite samples investigated in this study. The box for primary igneous carbonatites combines the fields as defined by [53,79]. Fresh and altered natrocarbonatites are shown for comparison (KH95=Data from [50]). The field labeled “Lengai” defines the C–O isotopic compositions of fresh natrocarbonatites from Oldoinyo Lengai (after [53]). Analytical uncertainty is smaller than symbol size.

5.3. Li isotopic composition of the Oldoinyo Lengai mantle source

Unaltered natrocarbonatites from Oldoinyo Lengai, which have Li isotopic compositions falling within the range of mantle-derived basalts, are considered to reflect the $\delta^7\text{Li}$ of their mantle source. Moreover, the high Li concentrations (>200 ppm) of the carbonatites make it very difficult to shift their $\delta^7\text{Li}$ via bulk crustal assimilation, since typical crustal rocks have Li concentrations below 50 ppm [20,60] with averages of 35 ± 11 ppm and 13 ppm for upper and lower crustal rocks, respectively [20,61]. Moreover, the low magmatic temperatures of natrocarbonatites (<600 °C) do not favor crustal assimilation so that even the occurrence of crustal rocks or minerals unusually rich in Li (e.g. granites containing up to 187 ppm [20] or biotites with 105 to 426 ppm Li [62]) are unlikely to significantly alter their $\delta^7\text{Li}$. The similarity of the carbonatite, melilitite and nephelinite Li isotope ratios to those of MORB, OIB and intracontinental basalts (Fig. 2) suggests that their Li budget derives from similar sources and/or processes. Thus, whatever Li isotope heterogeneities may exist in the mantle source regions, appear to be homogenized during melt generation and melt transport, at least at the scale of $\pm 2\%$.

The distinctly lighter Li isotope composition of the phonolite compared to the other samples may be produced by several distinct processes such as weathering, metasomatism of the mantle source region or crustal assimilation. Weathering is known to lower $\delta^7\text{Li}$ values [24], but there is neither chemical evidence for weathering, since major, trace and fluid-mobile element data (Rb, Ba) of this sample follow the general patterns of the Lengai lavas [35], nor do petrographic observations suggest weathering. Although the presence of a low- $\delta^7\text{Li}$ EM1-like metasomatic mantle component has been suggested by Nishio et al. [17], more recent investigations [18] show that the low $\delta^7\text{Li}$ values in these pyroxenes are caused by isotopic fractionation via diffusion and are ephemeral. Ocean islands with EM1 affinities also do not have anomalously low $\delta^7\text{Li}$ [11], so there is considerable doubt about the existence of an exotic low- $\delta^7\text{Li}$ mantle reservoir. A more likely explanation for the low $\delta^7\text{Li}$ of the phonolite is that it reflects assimilation of isotopically light continental crust. Previous studies have suggested that the phonolites formed by crystal fractionation and crustal contamination of olivine nephelinitic magma [43], and assimilation of mafic lower crustal granulites was proposed on the basis of Sr–Nd–Pb radiogenic isotope data [51]. Average lower crustal granulites have 8 ppm Li and $\delta^7\text{Li}$ of 0, but range as low

as -18 [60]. If we assume a lower crustal contaminant with 8 ppm Li and $\delta^7\text{Li} = -9$, the phonolite composition can be modeled by 20% assimilation — fractional crystallization from a parent magma with $\delta^7\text{Li} = +3.5$ and 10 ppm Li (Fig. 6). Thus, crustal assimilation is a viable process to explain the lower $\delta^7\text{Li}$ in the phonolite, but it remains hypothetical until more Li compositional data of both phonolites and the lower crust beneath Tanzania are available.

5.4. Fractionation of Li isotopes during magmatic differentiation

In the absence of experimental data on Li isotope fractionation between minerals and melts at magmatic temperatures, the study of co-genetic magmatic rocks provides a means to evaluate Li isotope fractionation during differentiation. The lack thereof has been demonstrated for basalts and their constituent minerals [9,10] and co-genetic basaltic andesites, dacites and rhyolites [63]. The overlap of Li isotopic ratios of the olivine melilitites, considered to represent parental melts at Oldoinyo Lengai [34,43], with both the highly differentiated nephelinite and the natrocarbonatites suggests that the melt is not affected by significant Li isotopic fractionation during differentiation of these lavas. The highly differentiated composition of the natrocarbonatites may reflect ~ 60 wt. % fractional crystallization from a hypothetical primary sodic dolomitic carbonatite [64]. Li isotopic compositions are constant over a wide range of eruption temperatures (>1130 °C to ~ 500 °C,

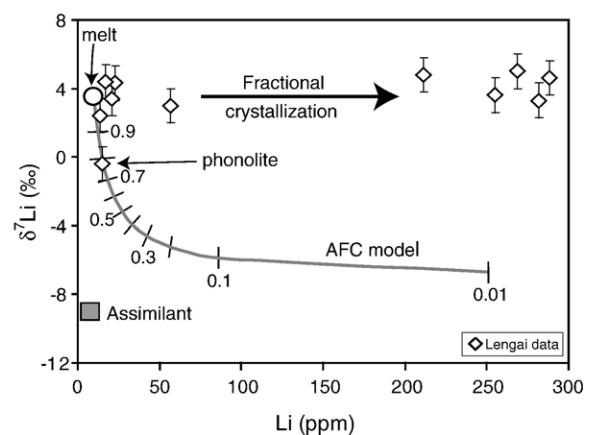


Fig. 6. Assimilation – fractional crystallization (AFC) modeling (after [80]) to explain the composition of the phonolite (OL 822). Parameters used: r (rate of assimilation/rate of crystallization) = 0.7, c_{Li} (hypothetical parental melt) = 10 ppm, c_{Li} (assimilant) = 8 ppm (average of granulites), $\delta^7\text{Li}_{\text{melt}} = +3.5$, $\delta^7\text{Li}_{\text{assimilant}} = -9$, $D_{\text{Li}}^{\text{solid/liquid}} = 0.2$. Numbers at model curve reflect the fraction of melt remaining.

Fig. 7). This is consistent with previous studies that documented the absence of significant Li isotope fractionation during moderate degrees of magmatic differentiation at high (>1150 °C [9,10]) to moderate (800–720 °C [20]) temperatures.

5.5. Li isotope fractionation between whole-rocks and phenocrysts

The light Li isotopic composition of clinopyroxenes compared to their respective whole-rocks (Fig. 3) indicates a lack of equilibration between the two. In the olivine melilitite (OL 352) and the nephelinite (OL 804), the concentration of Li in clinopyroxene is low compared to the whole-rock. The modal proportion of clinopyroxene is also low (<5%), so that clinopyroxene does not have a significant influence on the Li isotopic composition of the whole-rock. In contrast, the phonolite contains a significantly higher proportion of clinopyroxene (~30%) that has a relatively high Li content. Therefore, clinopyroxene is expected to exert a significant control on the whole-rock Li budget, consistent with the observed small difference between whole-rock and mineral isotope values. Different sample preparation techniques for mineral separates can influence the Li isotopic composition [56], but the gentle ultrasonic cleaning in Milli-Q water chosen for the clinopyroxenes of this study was shown to give the most reliable results [14,56]. Moreover, if contamination from the whole-rock had not been effectively removed from the clinopyroxenes, one would expect their $\delta^7\text{Li}$ values to be closer to the whole-rock value, but not

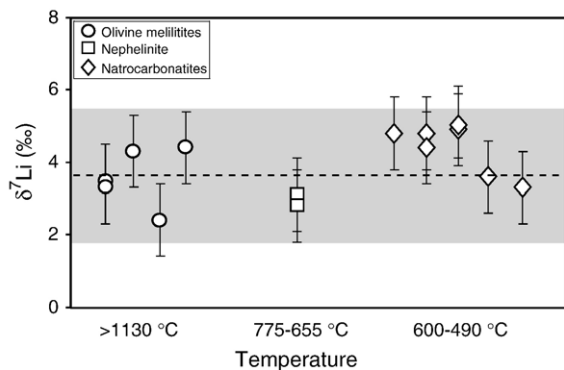


Fig. 7. Plot of $\delta^7\text{Li}$ vs. temperature in Oldoinyo Lengai rocks. Temperature estimates are after [31] for olivine melilitites, [44,46] for nephelinite and [32,33] for carbonatites. The dashed line and the grey bar represent the average $\delta^7\text{Li}$ value of the olivine melilitites and its 2σ standard deviation (3.6 ± 1.9). Note that the range in $\delta^7\text{Li}$ of the olivine melilitites completely overlaps with analyses of recent MORB samples (cf. Fig. 2).

distinctly lower. Thus, the low $\delta^7\text{Li}$ values of the clinopyroxenes appear to be real and need to be explained. Equilibrium isotope fractionation between melt and clinopyroxenes is excluded because the isotope fractionation in the highest temperature lava (OL 352, olivine melilitite) is greater than in the lower temperature lavas, contrary to expectation, i.e., diminishing fractionation at higher temperatures.

Recent experimental studies have shown that Li diffusion in silicate melts and minerals is very rapid [65–67] and can generate large concentration and isotopic gradients [27,28]. Moreover, diffusion-driven isotopic fractionation can occur at high temperatures where equilibrium fractionation diminishes [68]. If Li continues to diffuse from the melt into the clinopyroxene/olivine phenocrysts during final ascent and cooling of the lava [69], the phenocrysts will be relatively enriched in ^6Li because ^6Li diffuses faster than ^7Li [27,65]. The intermediate $\delta^7\text{Li}$ value of olivine, between whole-rock and clinopyroxene, and the lower Li content of olivine compared to clinopyroxene, could reflect a slower diffusion of Li in olivine compared to pyroxene, but more data are necessary to evaluate the relative diffusivities of these two minerals. Diffusion would only occur if a driving mechanism exists. For example, a change in chemical potential for lithium between clinopyroxene and melt due to cooling could occur if the partition coefficient $D^{\text{cpx-melt}}$ for Li increases with decreasing temperature, which would cause Li to diffuse from the melt into the crystal upon cooling. Unfortunately, relevant partitioning data for Li are not available. An alternative driving mechanism is the preferential partitioning of Li into pyroxene compared to groundmass phases at sub-solidus conditions [70], which has been demonstrated experimentally for feldspar [67]. In that case, the groundmass would crystallize from a relative Li-rich intercumulus liquid, and diffusion could occur by an interstitial mechanism [66] from the groundmass phases into the pyroxene.

Flat- and U-shaped abundance patterns for Li concentrations in pyroxenes from Martian meteorites are in accordance with diffusion modeling [70]. Clinopyroxenes and olivines from Oldoinyo Lengai have variable and generally non-systematic distributions of Li concentrations (Table 2). The absence of any correlation between the Li concentrations and other compositional characteristics in these minerals argues against an origin by magmatic fractionation (Fig. 4). Even though we do not find evidence for diffusive controlled processes in the Li abundance profiles, it has been shown that Li isotopic compositions may vary even in grains where Li abundance patterns are flat [70]. Therefore,

diffusion may well have caused the Li isotopic variability in the mineral separates compared to the whole-rocks.

The feasibility of diffusion causing lighter Li isotopic composition in phenocryst minerals is explored using a one-dimensional diffusion model equation [71], assuming that the melt is an infinite Li reservoir relative to the mineral:

$$[(C_x - C_1)/(C_0 - C_1)] = \operatorname{erfc}[x/2(Dt)^{0.5}],$$

with x = distance into the crystal [m], C_x = element concentration at distance x , C_0 = element concentration in the melt, C_1 = element concentration in the crystal, D = diffusion coefficient [$\text{m}^2 \text{s}^{-1}$], t = time and erfc = complementary error function. This model has been successfully used to model Li diffusion from a pegmatite into country rocks [28]. The diffusion curves are modeled separately for ^6Li and ^7Li , and the resulting $^7\text{Li}/^6\text{Li}$ ratio is calculated by combining the concentrations at different distances [28]. In our example, $C_0 = 30$ ppm, $C_1 = 7$ ppm and $\delta^7\text{Li} = +4.0$ at the melt-crystal interface were chosen to approximate conditions applicable for the silicate samples. Diffusion coefficients of 4.6×10^{-12} and $5 \times 10^{-15} \text{ m}^2 \text{ s}^{-1}$, as determined experimentally for clinopyroxene [67], were chosen to reflect temperatures of 1100 °C to 800 °C. To model the $\delta^7\text{Li}$ curve, we follow [68] in assuming that the ratio of the effective diffusion coefficients for the light (1) and heavy (2) isotopes of an element i are related to their mass according to the equation: $D_{i,1}/D_{i,2} = (m_{i,2}/m_{i,1})^\beta$. The value of the empirical parameter β was chosen to be 0.215 after [65]. The size of clinopyroxene is based on its occurrence as >0.1 mm phenocrysts in all Oldoinyo Lengai silicate lavas (see Appendix). The results (Fig. 8a) show that diffusion profiles in pyroxene always evolve to very light Li isotopic compositions, down to -11% . Although the time scales of evolution for the silicate magmas are not known, U–Th disequilibria have shown a mean magma reservoir lifetime of 10–15 years for natrocarbonatite lavas erupted in 1960–1963 [72]. At a temperature of 800 °C, broadly reflecting the temperature of carbonated silicate parent magmas to the natrocarbonatites [46], diffusion profiles yielding very light $\delta^7\text{Li}$ values can be retained for this time and longer. At higher temperatures, more relevant to the genesis of the olivine melilitite, light $\delta^7\text{Li}$ values can still be retained for several weeks. Modeled Li concentration profiles reflecting diffusion between an olivine melilitite groundmass and an olivine phenocryst (Fig. 8b) show a steep Li decrease for rapidly cooled samples. The calculated profiles agree

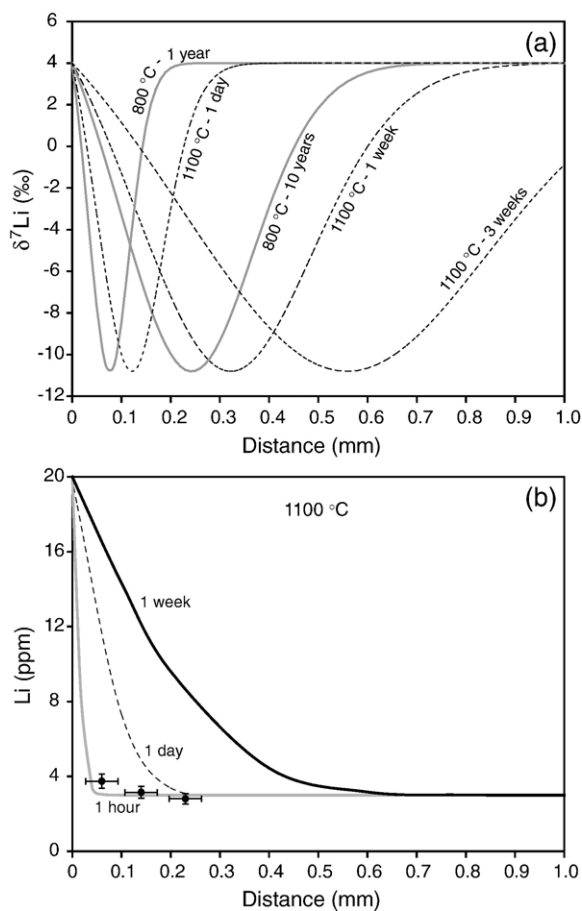


Fig. 8. Diffusion modeling, using a one-dimensional diffusion model equation [71] and diffusion coefficients from [67] (see text for discussion): (a) Model showing Li isotope fractionation by diffusion in clinopyroxene, modeled with a Li concentration in the surrounding melt of 30 ppm, an original Li concentration in the pyroxene of 7 ppm and $\delta^7\text{Li} = +4.0$ at the melt-crystal interface. Diffusion coefficients for temperatures of 800 °C (solid gray lines) and 1100 °C (dashed lines) were used. (b) Model reflecting Li diffusion between olivine melilitite melt (Li = 20 ppm) and olivine (Li = 3 ppm) at 1100 °C for various time scales. The assumed diffusion coefficient is taken to be similar to the one for clinopyroxene, since Li diffusion coefficients for olivine are not known. The black points are 3 data points from the olivine crystal in Fig. 4.

well with the one measured, taking into account uncertainties in both model parameters and spatial resolution of the measurement. In summary, the modeling shows that light Li isotopic compositions can occur in phenocrysts over a wide range of temperatures and diffusion time. It is therefore likely that parts of the phenocrysts retain a light Li isotopic composition when the magma is erupted and rapidly cooled, thus leading to an overall lighter Li isotopic signature in the mineral separates.

6. Conclusions

The conclusions of this study are as follows:

1. Natrocarbonatite lavas of Oldoinyo Lengai possess high Li concentrations (>200 ppm), mostly due to small degrees of melting and prolonged differentiation. The carbonatites are ~5.5 times more enriched than conjugate, highly differentiated nephelinites, suggesting a preference of Li for the carbonatite melt during liquid immiscibility.
2. The Li isotopic composition of Oldoinyo Lengai natrocarbonatites reflect the values of their mantle source, which is similar to that of MORB, OIB and intracontinental basalts. This suggests that the mantle may be fairly homogeneous in terms of its Li isotope composition. Alternatively, Li isotope heterogeneities that may exist in the mantle are homogenized during melt generation and ascent.
3. There is no indication for the involvement of an EM1-like component with extremely low $\delta^7\text{Li}$ in the petrogenesis of the OL rocks, despite the fact that an EM-1 component is implicated in their genesis on the basis of Sr–Nd–Pb isotope compositions [51]. This is consistent with published Li isotope data for EM-1-like intraplate basalts, which show $\delta^7\text{Li}$ similar to MORB and other OIB [11].
4. The lack of per mil level differences in $\delta^7\text{Li}$ between primitive lavas (olivine melilitites) and highly differentiated lavas (nephelinite, carbonatites) suggests that there is no or very little Li isotope fractionation during magmatic differentiation from temperatures >1100 °C to 500 °C.
5. Isotopic differences between whole-rocks and clinopyroxene/olivine phenocrysts are interpreted to reflect isotope fractionation caused by diffusion of Li from the magma into the phenocryst during eruption and cooling of the lavas.

Acknowledgements

We thank F.-Z. Teng, M. Marks, R. Ash and P. Piccoli for help and advice with sample processing, ICP-MS, MC-ICP-MS and electron microprobe measurements, and K. Simon for providing some preliminary Li concentration data. A.J. Kaufmann and N. Collins are thanked for their help with C and O isotope analyses. K. Bell kindly provided samples from the 1993 eruption. Constructive reviews by H.-M. Seitz and an anonymous referee and careful editing by R. Carlson greatly improved the manuscript. A Feodor–Lynen fellowship to R.H. by the Humboldt foundation is gratefully acknowl-

edged. This work was also supported by the N.S.F. (EAR 0208012).

Appendix A

Sample description of Oldoinyo Lengai lavas (coordinates in UTM-grid (ARC 1960)):

OL 123: Natrocarbonatite, flow from hornito T37, Oct 1995

Location: active North crater, S2°45.4/E 35°54.8

Texture: highly porphyritic, almost no interstitial matrix

Mineralogy: Nyerereite and Gregoryite (max 1–2 mm) phenocrysts; quenched matrix with intergrowth of Na-carbonates, fluorite and sylvite

OL 148, OL 259: Natrocarbonatite, flows from hornito T49, Oct 3rd and Oct 9th 2000, respectively

Location: active North crater, S2°45.4/E 35°54.8

Texture: porphyritic

Mineralogy: Nyerereite and Gregoryite (max 1–2 mm) phenocrysts; quenched matrix with intergrowth of Na-carbonates, fluorite and sylvite

OL 352: Olivine melilitite

Location: Sinja-Eledei Canyon, S2°44.21/E 35°59.15

Type: Lava block within lahar deposit

Texture: porphyritic

Mineralogy: olivine (<3 mm), melilite (<600 μm), cpx (<2 mm) and perovskite (<300 μm) phenocrysts; groundmass: melilite, magnetite, perovskite, cpx, nepheline

OL 198, OL 343: Olivine melilitites

Location: Dorobo Cone, S2°44.4/E 35°56.6

Type: Lava blocks within debris-flow unit

OL 12/12K: Olivine melilitite

Location: Armykon Hill at the south shore of Lake Natron, S2°36.0/E 35°54.6

Type: Black glassy lava flow

OL 804: Combeite wollastonite nephelinite (CWN), Lengai II B unit

Location: Upper N-Flank, S2°45.17/E35°54.96

Type: Lava flow

Texture: porphyritic

Mineralogy: nepheline (<3 mm), cpx (<1.5 mm) and Ti-garnet (<1 mm) phenocrysts; nepheline, combeite, wollastonite and cpx (all 300–400 μm) microphenocrysts; groundmass: cpx, apatite

OL 822: Phonolite, Lengai I unit

Location: Lower E-Flank, Eastern Chasm, S2°45.05/E35°56.06

Type: Lava flow

Structure: porphyritic, flow texture

Mineralogy: nepheline (<3 mm), cpx (<1.5 mm) and titanite (<1.5 mm) phenocrysts; nepheline, sanidine,

titanite, cpx and sodalite microphenocrysts; groundmass: nepheline, cpx

OL-2, OL-7: Natrocarbonatites, flows from hornito T23, June 29th, 1993

Location: Active North crater, S2°45.4/E 35°54.8

References

- [1] J.G. Ryan, C.H. Langmuir, The systematics of lithium abundances in young volcanic rocks, *Geochim. Cosmochim. Acta* 51 (1987) 1727–1741.
- [2] P.B. Tomascak, Developments in the understanding and application of lithium isotopes in the Earth and planetary sciences, in: C. Johnson, B. Beard, F. Albarede (Eds.), *Geochemistry of Non-Traditional Stable Isotopes*, vol. 55, Mineralogical Society of America, Washington, DC, 2004, pp. 153–195.
- [3] T. Elliott, A. Jeffcoate, C. Bouman, The terrestrial Li isotope cycle: light-weight constraints on mantle convection, *Earth Planet. Sci. Lett.* 220 (2004) 231–245.
- [4] T. Elliott, A. Thomas, A. Jeffcoate, Y. Niu, Lithium isotope evidence for subduction-enriched mantle in the source of mid-ocean-ridge basalts, *Nature* 443 (2006) 565–568.
- [5] L.-H. Chan, J.M. Edmond, G. Thompson, K. Gillis, Lithium isotopic composition of submarine basalts: implications for lithium cycle in the oceans, *Earth Planet. Sci. Lett.* 108 (1992) 151–160.
- [6] T. Moriguti, E. Nakamura, Across-arc variation of Li isotopes in lavas and implications for crust/mantle recycling at subduction zones, *Earth Planet. Sci. Lett.* 163 (1998) 167–174.
- [7] P.B. Tomascak, C.H. Langmuir, P.J. le Roux, S.B. Shirey, Lithium isotopes in global mid-ocean ridge basalts, *Geochim. Cosmochim. Acta*, submitted for publication.
- [8] G.D. Flesch, A.R.J. Anderson, H.J. Svec, A secondary isotopic standard for $^6\text{Li}/^7\text{Li}$ determinations, *Int. J. Mass Spectrom. Ion Process.* 12 (1973) 265–272.
- [9] L.-H. Chan, F.A. Frey, Lithium isotope geochemistry of the Hawaiian plume: results from the Hawaii Scientific Drilling Project and Koolau Volcano, *Geochem. Geophys. Geosyst.* 4 (3) (2003) 8707, doi:10.1029/2002GC000365.
- [10] P.B. Tomascak, F. Tera, R.T. Helz, R.J. Walker, The absence of lithium isotope fractionation during basalt differentiation: new measurements by multicollector sector ICP-MS, *Geochim. Cosmochim. Acta* 63 (1999) 907–910.
- [11] J.G. Ryan, P.R. Kyle, Lithium abundance and lithium isotope variations in mantle sources: insights from intraplate volcanic rocks from Ross Island and Marie Byrd Land (Antarctica) and other oceanic islands, *Chem. Geol.* 212 (2004) 125–142.
- [12] Y. Nishio, S. Nakai, T. Kogiso, H.G. Barszczus, Lithium, strontium, and neodymium isotopic compositions of oceanic island basalts in the Polynesian region: constraints on a Polynesian HIMU origin, *Geochem. J.* 39 (2005) 91–103.
- [13] P.B. Tomascak, J.G. Ryan, M.J. Defant, Lithium isotope evidence for light element decoupling in the Panama subarc mantle, *Geology* 28 (2000) 507–510.
- [14] T. Zack, P.B. Tomascak, R.L. Rudnick, C. Dalpé, W.F. McDonough, Extremely light Li in orogenic eclogites: the role of isotope fractionation during dehydration in subducted oceanic crust, *Earth Planet. Sci. Lett.* 208 (2003) 279–290.
- [15] R.L. Romer, W. Heinrich, B. Schröder-Smeibidl, A. Meixner, C.-O. Fischer, C. Schulz, Elemental dispersion and stable isotope fractionation during reactive fluid-flow and fluid-immiscibility in the Burfa del Diente aureole, NE-Mexico: evidence from radiographies and Li, B, Sr, Nd, and Pb isotope systematics, *Contrib. Mineral. Petrol.* 149 (2005) 400–429.
- [16] R.A. Brooker, R.H. James, J.D. Blundy, Trace elements and Li isotope systematics in Zabargad peridotites: evidence of ancient subduction processes in the Red Sea mantle, *Chem. Geol.* 212 (2004) 179–204.
- [17] Y. Nishio, S. Nakai, J. Yamamoto, H. Sumino, T. Matsumoto, V.S. Prikhod'ko, S. Arai, Lithium isotopic systematics of the mantle-derived ultramafic xenoliths: implications for EM1 origin, *Earth Planet. Sci. Lett.* 217 (2004) 245–261.
- [18] R. Rudnick, D.A. Ionov, Lithium elemental and isotopic disequilibrium in minerals from peridotite xenoliths from far-east Russia: product of recent melt/fluid-rock reaction, *Earth Planet. Sci. Lett.*, submitted for publication.
- [19] C.J. Bryant, B.W. Chappell, V.C. Bennett, M.T. McCulloch, Lithium isotopic composition of the New England Batholith: correlations with inferred source rock compositions, *Trans. R. Soc. Edinb. Earth Sci.* 95 (2004) 199–214.
- [20] F.-Z. Teng, W.F. McDonough, R.L. Rudnick, C. Dalpé, P.B. Tomascak, B.W. Chappell, S. Gao, Lithium isotopic composition and concentration of the upper continental crust, *Geochim. Cosmochim. Acta* 68 (2004) 4167–4178.
- [21] F.-Z. Teng, W.F. McDonough, R.L. Rudnick, R. Walker, M.-L.C. Sirbescu, Lithium isotopic systematics of granites and pegmatites from the Black Hills, South Dakota, *Am. Mineral.* 91 (2006) 1488–1498.
- [22] L.-H. Chan, J.M. Edmond, G. Thompson, A lithium isotope study of hot springs and metabasalts from mid-ocean ridge hydrothermal systems, *J. Geophys. Res.* 98 (1993) 9653–9659.
- [23] W.E. Seyfried, X. Chen, L.-H. Chan, Trace element mobility and lithium isotope exchange during hydrothermal alteration of seafloor weathered basalt: an experimental study at 350 °C, 500 bars, *Geochim. Cosmochim. Acta* 62 (1998) 949–960.
- [24] R.L. Rudnick, P.B. Tomascak, B.N. Heather, L.R. Gardner, Extreme lithium isotopic fractionation during continental weathering revealed in saprolites from South Carolina, *Chem. Geol.* 212 (2004) 45–57.
- [25] B. Kiskirek, M. Widdowson, R.H. James, Behavior of Li isotopes during continental weathering: the Bidar laterite profile, India, *Chem. Geol.* 212 (2004) 27–44.
- [26] L.D. Benton, J.G. Ryan, I.P. Savov, Lithium abundance and isotope systematics of forearc serpentinites, Conical Seamount, Mariana forearc: insights into the mechanics of slab-mantle exchange during subduction, *Geochem. Geophys. Geosyst.* 5 (2004), doi:10.1029/2004GC000708 (Q08J12).
- [27] C.C. Lundstrom, M. Chaussidon, A.T. Hsui, P. Kelemen, M. Zimmermann, Observations of Li isotopic variations in the Trinity Ophiolite: evidence for isotopic fractionation by diffusion during mantle melting, *Geochim. Cosmochim. Acta* 69 (2005) 735–751.
- [28] F.-Z. Teng, W.F. McDonough, R.L. Rudnick, R.J. Walker, Diffusion-driven lithium isotopic fractionation in country rocks of the Tin Mountain pegmatite, *Earth Planet. Sci. Lett.* 243 (2006) 701–710.
- [29] P. Beck, J.A. Barrat, M. Chaussidon, P. Gillet, M. Bohn, Li isotopic variations in single pyroxenes from the Northwest Africa 480 shergottite (NWA 480): a record of degassing of Martian magmas? *Geochim. Cosmochim. Acta* 68 (2004) 2925–2933.
- [30] K. Bell, G.R. Tilton, Nd, Pb and Sr isotopic compositions of East African Carbonatites: evidence for mantle mixing and plume inhomogeneity, *J. Petrol.* 42 (2001) 1927–1945.

- [31] F.E. Lloyd, Experimental melting and crystallisation of glassy olivine melilitites, *Contrib. Mineral. Petrol.* 90 (1975) 236–243.
- [32] M. Krafft, J. Keller, Temperature measurements in carbonatite lava-lakes and flows: Oldoinyo Lengai, Tanzania, *Science* 245 (1989) 168–170.
- [33] H. Pinkerton, G.E. Norton, J.B. Dawson, D.M. Pyle, Field observations and measurements of the physical properties of Oldoinyo Lengai alkali carbonatite lavas, November 1988, in: K. Bell, J. Keller (Eds.), *Carbonatite Volcanism: Oldoinyo Lengai and the Petrogenesis of Natrocarbonatites*, Springer, Berlin, 1995, pp. 23–36.
- [34] J. Keller, A.N. Zaitsev, D. Wiedenmann, Primary magmas at Oldoinyo Lengai: the role of olivine melilitites, *Lithos* 91 (2006) 150–172.
- [35] J. Klaudius, J. Keller, Peralkaline silicate lavas at Oldoinyo Lengai (Tanzania), *Lithos* 91 (2006) 173–190.
- [36] A. Simonetti, K. Bell, C. Shradly, Trace- and rare-earth-element geochemistry of the June 1993 natrocarbonatite lavas, Oldoinyo Lengai (Tanzania): implications for the origin of carbonatite magmas, *J. Volcanol. Geotherm. Res.* 75 (1997) 89–106.
- [37] H.P. Qi, P.D.P. Taylor, M. Berglund, P. De Bièvre, Calibrated measurements of the isotopic composition and atomic weight of the natural Li isotopic reference material IRMM-016, *Int. J. Mass Spectrom. Ion Process.* 171 (1997) 263–268.
- [38] R.H. James, M.R. Palmer, The lithium isotope composition of international rock standards, *Chem. Geol.* 166 (2000) 319–326.
- [39] C. Bouman, T. Elliott, P.Z. Vroon, Lithium inputs to subduction zones, *Chem. Geol.* 212 (2004) 59–79.
- [40] N.J.G. Pearce, W.T. Perkins, J.A. Westgate, M.P. Gorton, E.E. Jackson, C.R. Neal, S.P. Chenery, A compilation of new and published major and trace element data for NIST SRM 610 and NIST SRM 612 glass reference materials, *Geostand. Newsl.* 21 (1997) 115–144.
- [41] <http://georem.mpch-mainz.gwdg.de/>
- [42] J.B. Dawson, H. Pinkerton, G.E. Norton, D.M. Pyle, P. Browning, D. Jackson, A.E. Fallick, Petrology and geochemistry of Oldoinyo Lengai lavas extruded in November 1988: magma source, ascent and crystallization, in: K. Bell, J. Keller (Eds.), *Carbonatite Volcanism: Oldoinyo Lengai and the Petrogenesis of Natrocarbonatites*, Springer, Berlin, 1995, pp. 47–69.
- [43] T.D. Peterson, B.A. Kjarsgaard, What are the parental magmas at Oldoinyo Lengai? in: K. Bell, J. Keller (Eds.), *Carbonatite Volcanism: Oldoinyo Lengai and the Petrogenesis of Natrocarbonatites*, Springer, Berlin, 1995, pp. 148–162.
- [44] T. Peterson, Peralkaline nephelinites. I. Comparative petrology of Shombole and Oldoinyo L'engai, East Africa, *Contrib. Mineral. Petrol.* 101 (1989) 458–478.
- [45] J. Keller, B. Spettel, The trace element composition and petrogenesis of natrocarbonatites, in: K. Bell, J. Keller (Eds.), *Carbonatite Volcanism: Oldoinyo Lengai and the Petrogenesis of Natrocarbonatites*, Springer, Berlin, 1995, pp. 70–86.
- [46] B.A. Kjarsgaard, D.L. Hamilton, T. Peterson, Peralkaline nephelinite/carbonatite liquid immiscibility: comparison of phase compositions in experiments and natural lavas from Oldoinyo Lengai, in: K. Bell, J. Keller (Eds.), *Carbonatite Volcanism: Oldoinyo Lengai and the Petrogenesis of Natrocarbonatites*, Springer, Berlin, 1995, pp. 163–190.
- [47] J.D. Twyman, J. Gittins, Alkalic carbonatite magmas: parental or derivative? in: J.G. Fitton, B.G.J. Upton (Eds.), *Alkaline Igneous Rocks*, Geological Society Special Publications, vol. 30, 1987, pp. 85–94.
- [48] V. Morogan, R.F. Martin, Mineralogy and partial melting of fenitized crustal xenoliths in the Oldoinyo Lengai carbonatite volcano, *Am. Mineral.* 70 (1985) 1114–1126.
- [49] T.F.D. Nielsen, I.V. Veksler, Is natrocarbonatite a cognate fluid condensate? *Contrib. Mineral. Petrol.* 142 (2002) 425–435.
- [50] J. Keller, J. Hoefs, Stable isotope characteristics of recent natrocarbonatites from Oldoinyo Lengai, in: K. Bell, J. Keller (Eds.), *Carbonatite Volcanism: Oldoinyo Lengai and the Petrogenesis of Natrocarbonatites*, Springer, Berlin, 1995, pp. 113–123.
- [51] K. Bell, A. Simonetti, Carbonatite magmatism and plume activity: implications from the Nd, Pb and Sr isotope systematics of Oldoinyo Lengai, *J. Petrol.* 37 (1996) 1321–1339.
- [52] K. Bell, J.B. Dawson, Nd and Sr isotope systematics of the active carbonatite volcano, Oldoinyo Lengai, in: K. Bell, J. Keller (Eds.), *Carbonatite Volcanism: Oldoinyo Lengai and the Petrogenesis of Natrocarbonatites*, Springer, Berlin, 1995, pp. 100–112.
- [53] J. Keller, A. Zaitsev, Calcicocarbonatite dykes at Oldoinyo Lengai, Tanzania: the fate of natrocarbonatite, *Can. Mineral.* 44 (2006) 857–876.
- [54] S.M. Eggins, R.L. Rudnick, W.F. McDonough, The composition of peridotites and their minerals: a laser-ablation ICP-MS study, *Earth Planet. Sci. Lett.* 154 (1998) 53–71.
- [55] H.-M. Seitz, A.B. Woodland, The distribution of lithium in peridotitic and pyroxenitic mantle lithologies — an indicator of magmatic and metasomatic processes, *Chem. Geol.* 166 (2000) 47–64.
- [56] H.-M. Seitz, G.P. Brey, Y. Lahaye, S. Durali, S. Weyer, Lithium isotopic signatures of peridotite xenoliths and isotopic fractionation at high temperature between olivine and pyroxenes, *Chem. Geol.* 212 (2004) 163–177.
- [57] L. Ottolini, B. Le Fèvre, R. Vannucci, Direct assessment of mantle boron and lithium contents and distribution by SIMS analyses of peridotite minerals, *Earth Planet. Sci. Lett.* 228 (2004) 19–36.
- [58] J.M. Brenan, E. Neroda, C.C. Lundstrom, H.F. Shaw, F.J. Ryerson, D.L. Phinney, Behaviour of boron, beryllium, and lithium during melting and crystallization: constraints from mineral-melt partitioning experiments, *Geochim. Cosmochim. Acta* 62 (1998) 2129–2141.
- [59] C.H. Donaldson, J.B. Dawson, R. Kanaris-Sotiriou, R.A. Batchelor, J.N. Walsh, The silicate lavas of Oldoinyo Lengai, Tanzania, *Neues Jahrb. Mineral. Abh.* 156 (1987) 247–279.
- [60] F.-Z. Teng, W.F. McDonough, R.L. Rudnick, S. Gao, P.B. Tomascak, Lithium isotopic systematics of high-grade metamorphic rocks: Implications for Li isotopic composition and concentration of the deep continental crust, *Geochim. Cosmochim. Acta*, submitted for publication.
- [61] R.L. Rudnick, S. Gao, Composition of the continental crust, In: The Crust. R.L. Rudnick (ed.), *Treatise on Geochemistry*, Vol. 3, H.D. Holland and K.K. Turekian (eds.), Oxford: Elsevier, 1–64, 2003.
- [62] A.P. Jones, J.V. Smith, Ion probe analysis of H, Li, B, F and Ba in micas, with additional data for metamorphic amphibole, scapolite and pyroxene, *N. Jb. Mineral. Mh.* 5 (1984) 228–240.
- [63] T. Magna, U. Wiechert, T.L. Grove, A.N. Halliday, Lithium isotope fractionation in the southern Cascadia subduction zone, *Earth Planet. Sci. Lett.* 250 (2006) 428–443, doi:10.1016/j.epsl.2006.08.019.
- [64] R.J. Sweeney, T.J. Falloon, D.H. Green, Experimental constraints on the possible mantle origin of natrocarbonatite, in: K. Bell, J. Keller (Eds.), *Carbonatite Volcanism: Oldoinyo Lengai and the Petrogenesis of Natrocarbonatites*, Springer, Berlin, 1995, pp. 191–207.
- [65] F.M. Richter, A.M. Davis, D.J. DePaolo, E.B. Watson, Isotope fractionation by chemical diffusion between molten basalt and rhyolite, *Geochim. Cosmochim. Acta* 67 (2003) 3905–3923.

- [66] B.J. Giletti, T.M. Shanahan, Alkali diffusion in plagioclase feldspar, *Chem. Geol.* 139 (1997) 3–20.
- [67] L.A. Coogan, S.A. Kasemann, S. Chakraborty, Rates of hydrothermal cooling of new oceanic upper crust derived from lithium-geospeedometry, *Earth Planet. Sci. Lett.* 240 (2005) 415–424.
- [68] F.M. Richter, Y. Liang, A.M. Davis, Isotope fractionation by diffusion in molten oxides, *Geochim. Cosmochim. Acta* 63 (1999) 2853–2861.
- [69] A.B. Jeffcoate, T. Elliott, S.A. Kasemann, D. Ionov, K. Cooper, R. Brooker, Li isotope fractionation in peridotites and mafic melts, *Geochim. Cosmochim. Acta*, in press.
- [70] P. Beck, M. Chaussidon, J.A. Barrat, P. Gillet, M. Bohn, Diffusion induced Li isotopic fractionation during the cooling of magmatic rocks: the case of pyroxene phenocrysts from nakhlite meteorites, *Geochim. Cosmochim. Acta* 70 (2006) 4813–4825.
- [71] J. Crank, *The Mathematics of Diffusion*, Clarendon Press, Oxford, 1975.
- [72] D.M. Pyle, Decay series evidence for transfer and storage times of natrocarbonatite magma, in: K. Bell, J. Keller (Eds.), *Carbonatite Volcanism: Oldoinyo Lengai and the Petrogenesis of Natrocarbonatites*, Springer, Berlin, 1995, pp. 124–136.
- [73] W.P. Leeman, S. Tonarini, L.-H. Chan, L.E. Borg, Boron and lithium isotopic variations in a hot subduction zone — the southern Washington Cascades, *Chem. Geol.* 212 (2004) 101–124.
- [74] P.B. Tomascak, E. Widom, L.D. Benton, S.L. Goldstein, J.G. Ryan, The control of lithium budgets in island arcs, *Earth Planet. Sci. Lett.* 196 (2002) 227–238.
- [75] E. Jagoutz, H. Palme, H. Baddenhausen, K. Blum, M. Cendales, G. Dreibus, B. Spettel, V. Lorenz, H. Wänke, The abundances of major, minor and trace elements in the earth's mantle as derived from primitive ultramafic nodules, *Proc. Lunar Planet. Sci. Conf. 10th* (1979) 2031–2050.
- [76] T. Moriguti, T. Shibata, E. Nakamura, Lithium, boron and lead isotope and trace element systematics of Quaternary basaltic volcanic rocks in northeastern Japan: mineralogical controls on slab-derived fluid composition, *Chem. Geol.* 212 (2004) 81–100.
- [77] K. Kobayashi, R. Tanaka, T. Moriguti, K. Shimizu, E. Nakamura, Lithium, boron, and lead isotope systematics of glass inclusions in olivines from Hawaiian lavas: evidence for recycled components in the Hawaiian plume, *Chem. Geol.* 212 (2004) 143–161.
- [78] A.W. Hofmann, Mantle geochemistry: the message from oceanic volcanism, *Nature* 385 (1997) 219–229.
- [79] H.P. Taylor, J. Frechen, E.T. Degens, Oxygen and carbon isotope studies of carbonatites from the Laacher See district, West Germany and the Alnö district, Sweden, *Geochim. Cosmochim. Acta* 31 (1967) 407–430.
- [80] D.J. DePaolo, Trace element and isotopic effects of combined wallrock assimilation and fractional crystallization, *Earth Planet. Sci. Lett.* 53 (1981) 189–202.